Temporal Correlation in Cat Striate-Cortex Neural Spike Trains

Malvin C. Teich[1,2,3], Robert G. Turcott[3,4], and Ralph M. Siegel[5]

[1]Department of Electrical and Computer Engineering, Boston University
[2]Department of Biomedical Engineering, Boston University
[3]Department of Electrical Engineering, Columbia University
[4]School of Medicine, Stanford University
[5]Center for Molecular and Behavioral Neuroscience, Rutgers University

The existence of long-duration temporal correlation (i.e., memory) in the spike trains of certain sensory-system neurons is well established. Such correlation, extending to at least hundreds of seconds, has been demonstrated in cat retinal-ganglion (RGC) and lateral-geniculate (LGN) neurons [1, 2]; and in primary afferent auditory neurons of the cat [3-7], chinchilla [8], and chicken [9]. It is also present in the spike train of an insect visual interneuron, the descending contralateral movement detector (DCMD) of the locust [10]. Long-duration correlation is manifested at many levels in biological systems, from the microscopic to the macroscopic; examples include neurotransmitter exocytosis at the synapse [11] and fluctuations in the sequence of human heartbeats [12, 13]. In many cases, the upper limit of the observed correlation time is imposed by the duration of the recording.

In this article we draw on point-process theory and wavelet analysis to examine the variability and correlation properties of spike trains from single neurons in the cat striate cortex, under conditions of spontaneous and stimulated (driven) firing. It is not possible to infer the long-term correlation properties of a spike train from measures that reset at short times; thus, often-used spike-train measures, such as the interevent-interval histogram (IIH) and post-stimulus time (PST) histogram, cannot serve this purpose [14].

Rather, we make use of the event-number histogram (ENH), also called the spike-number or spike-count distribution. This measure affords the experimenter the opportunity of externally controlling the counting time, T, and therefore the duration over which spike correlations can be viewed. A useful and relatively simple gauge of the correlation properties is obtained from the first two moments of the ENH. In particular, the Fano factor (FF), defined as the ratio of the spike-count variance to the spike-count mean [15]:

$$F(T) = \mathrm{var}(N) / \overline{N} \qquad (1)$$

plotted as a function of the counting time, T, serves this purpose quite well. The FF is a special case of the wavelet Fano factor (WFF) implemented using the Haar wavelet basis [1].

Spike-number mean and variance measurements have been previously collected for visual-cortex neurons, both in the absence and in the presence of a stimulus. But they have always made use of a single, fixed counting time (typically ~ 1 s). Under these conditions, as summarized below, the FF generally lies between 1 and 5 (see Table 1). This is true whether the preparation is cat or monkey, anesthetized or unanesthetized, paralyzed or behaving; whether the cells are from striate or nonstriate cortex, simple or complex, spontaneously firing or stimulus-driven; and whether the independent stimulus variable is contrast, spatial frequency, or orientation.

However, the shape of the FF curve *as a function of the counting time* permits the nature of the temporal correlation to be determined [3, 4, 16]. We report Fano-factor curves for spontaneous and stimulus-driven striate-cortex spike trains over a broad range of counting times (10^{-3} s $\leq T \leq$ 770 s). Substantial long-duration correlation is present in all of them.

The unusual statistical properties inherent in the firing patterns of these neurons share some similarities with those observed from other sensory-system neurons, but the cortical-cell patterns are also unique in some respects. $F(T)$ clearly distinguishes spontaneous and driven neural firing patterns. In particular, the FFs for driven activity reveal several phenomena, some more well-known than others: quasirhythmic (so-called "40-Hz") activity, the presence of phase locking, and a reduction of fluctuations at very low frequencies relative to those present in spontaneous activity. Several other fea-

tures of the firing patterns emerge from our study.

Prior Measurements

In 1959, Hubel [17] qualitatively observed that the discharge of striate-cortex cells was highly irregular. In one of the earliest quantitative studies of cortical-cell statistics, in 1965, Smith and Smith [18] reported event-number histograms for cat forebrain cells that were light-responsive, but remote from the striate cortex. These researchers found that the action-potential occurrences were more clustered than expected according to the Poisson distribution, under both spontaneously firing and light-driven conditions. However, their measurements were conducted with a short counting (averaging) time fixed at $T = 50$ ms, so that the mean and variance they measured were necessarily small [13]. The actual values were not explicitly provided in their paper. Shortly thereafter, in 1966, Griffith and Horn [19] examined the mean firing rate and its fluctuations for spontaneously firing cat striate-cortex cells, again using a single averaging time (which in their case was based on the spontaneous firing rate of the cell). Qualitatively, the firing rate they observed exhibited long-term irregularities; these were particularly large for cells whose rate was determined using a large averaging time. However Griffith and Horn did not provide quantitative estimates for the magnitude of the fluctuations.

In an important study conducted a few years later in 1973, Sanseverino, et al. [20], obtained the mean firing rate, $\overline{R}$, and its standard deviation, σ_R, (using an averaging time $T = 1$ s) from 20-min recordings of cells in cat visual-cortex areas 17 (striate cortex), 18, and 19. Using the numerical values reported in their paper for $\overline{R}$ and σ_R, we have determined the FFs for three of their representative cells to be $F(T = 1\text{ s}) = 2.5$, 3.1, and 4.4, in areas 17, 18, and 19, respectively. (The measures used by Sanseverino, et al. [20], are readily converted to count mean and variance by using the relation $R = N/T$, where R is the firing rate and N is the number of spikes in the counting time T; thus, the mean firing rate, $\overline{R} = \overline{N}/T$, and $\text{var}(R) = \text{var}(N)/T^2$, so that $F(T) = \text{var}(N)/\overline{N} = T\,\text{Var}(R)/\overline{R} = T\sigma_R^2/\overline{R}$.) Schiller, et al. [21], subsequently showed that the response variability of simple and complex monkey striate-cortex cells (in their case, measured by the standard-deviation-to-mean ratio of the count, or event-number coefficient of variation, in a 1-s counting time), systematically decreased as deeper layers in the cortex were probed. Unfortunately, these researchers did not provide sufficient data in their paper to allow numerical values for the FF to be extracted.

The shape of the FF curve *as a function of the counting time* permits the nature of the temporal correlation to be determined.

A number of subsequent studies reported event-number variance versus mean measurements using T of the order of 1 s, and the results were all in substantial agreement with those of Sanseverino, et al. [20]. In particular, Tolhurst, et al. [22], obtained $F(T = \frac{1}{2}\text{ s}) \sim 3$-5 using 20-min data sets from anesthetized-cat striate-cortex simple and complex cells, using contrast as an independent variable. Dean [23] obtained $F(T = \frac{1}{2}\text{ s}) \sim 1.5$ using 50-s data sets from cat striate-cortex simple cells, using both spatial frequency and contrast as independent variables. Tolhurst, et al. [24], obtained $F(T = \frac{1}{4}$ or $\frac{1}{2}\text{ s}) \sim 3$ using 20-min data sets, and $F(T = \frac{1}{4}$ or $\frac{1}{2}\text{ s}) \sim 1.5$ using 5-min data sets, from cat simple and complex cells, again varying the contrast. Legéndy and Salcman [25] confirmed the bursty nature of the spontaneous firing patterns in unanesthetized-cat striate-cortex neurons, first observed by Hubel [17], but they did not report statistics for the event number. Bradley, et al. [26], obtained $F(T = \frac{1}{2}$ or 1 s) ~1.5 using 80-s data sets from anesthetized, paralyzed-cat complex cells, varying spatial frequency and contrast. Vogels, et al. [27], reported $F(T = 0.48\text{ s}) \sim 2$ using 10-min data sets from unanesthetized-monkey striate-cortex neurons while the

Table 1. Fano factor (spike-number variance-to-mean ratio) and conditions of measurement for various response-variability studies of visual-cortex neurons.

Year	Author	Cat/ Monkey	Spont/ Driven	Counting Time T (s)	Data-Length L (min)	Fano Factor $F(T)$
1959	Hubel	C	S/D			
1965	Smith & Smith	C	S/D	0.05		
1966	Griffith & Horn	C	S	5-33		
1973	Sanseverino, et al.	C	S	1	20	2-4.5
1976	Schiller, et al.	M	D	1	4	
1981	Tolhurst, et al.	C	D	½	20	3-5
1981	Dean	C	D	½	0.83	1.5
1983	Tolhurst, et al.	C/M C/M	D D	¼ or ½ ¼ or ½	20 5	3 1.5
1987	Bradley, et al.	C	D	½ or 1	1.33	1.5
1989	Vogels, et al.	M	D	0.48	10	2
1992	Snowden, et al.	M	D	1	selected segments	1-1.5
1993	Softky & Koch	M	D	1 or 2	selected segments	1-2
1996	**THIS PAPER**	C	S/D	0.001-770	5-128	1-80

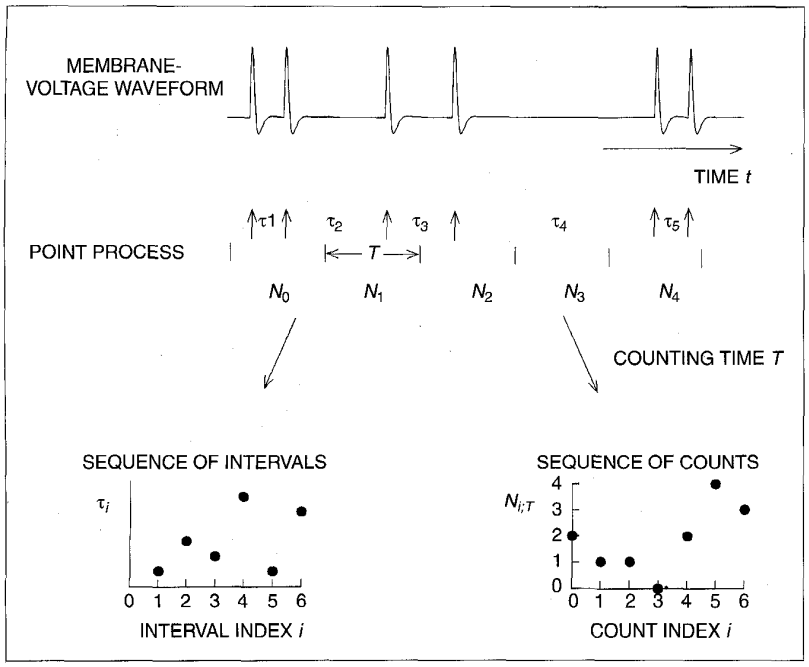

1. Stochastic processes used in the analysis of neural spike-train data. The continuous membrane-voltage waveform is idealized to a point process in which the occurrence times of action potentials are represented as unitary events (impulses) on the time axis. The sequence of interevent times is constructed from this point process by specifying the magnitude of each interval as a function of its index, thereby forming a positive real-valued discrete-time stochastic process. Real time is distorted in the formation of the sequence of intervals. The sequence of counts is constructed by specifying the number of nerve spikes (events) that occur in successive counting periods, each of duration T, as a function of the count index. The sequence of counts forms a positive integer-valued discrete-time stochastic process. Its time axis is directly related to that of the point process.

animal was performing an orientation-discrimination task. Snowden, et al. [28], observed $F(T = 1\text{ s}) \sim 1.1$ for striate-cortex neurons and $F(T = 1\text{ s}) \sim 1.4$ for middle-temporal (MT) visual-cortex neurons in the awake behaving monkey in response to random dot patterns, but these estimates were determined from brief action-potential segments. Most recently, in 1993, Softky and Koch [29] obtained $F(T = 1\text{ s}) \sim 1$ for striate-cortex neurons and $F(T = 2\text{ s}) \sim 2$ for MT visual-cortex neurons in the awake behaving monkey; however, their estimates were determined from action-potential segments selected for "constant firing rate." Such selection artificially suppresses long-duration correlation and results in a reduction of the observed variance and FF, as discussed subsequently (and illustrated in Fig. 3).

Statistical Methods

It is generally accepted that the occurrence times of the action potentials carry all of the information contained in a spike train. For purposes of analysis, therefore, a sequence of idealized impulses (a point process) is formed from the continuous waveform of the membrane voltage, as shown in the upper portion of Fig. 1.

The construction of two useful subsidiary processes, the sequence of intervals and the sequence of counts (event numbers) [30], is illustrated in the lower portion of Fig. 1.

Sequence of Intervals

The sequence of intervals is used to calculate interval-based statistical measures such as the interevent-interval histogram [30], the joint interevent-interval histogram [31] (also called the interval return map; see [32]), and the interval-based periodogram [13]. This sequence is a random process that has an amplitude specifying the magnitude of the interevent interval and an abscissa specifying the interval index. One inconvenient aspect of the sequence of intervals is the distortion of real time that occurs in the mapping from the point process to the abscissa; the interval index increases by unity whether the interval is long or short. Interval-based statistics are most often used to investigate the short-term behavior of a spike train [13].

Sequence of Counts

The sequence of counts is used for count-based statistical measures such as the rate function, event-number histogram [14, 30], and count-based periodogram [13, 30]. This sequence is also a random process, but with an amplitude given by the number of events in (usually contiguous) counting times of duration T, and the abscissa is the count index. In this case, the real time of the point process is preserved in the mapping to the sequence, since the count index increases by unity for every T seconds in the point process. As a result, the interpretation of count-based correlation measures is straightforward.

Fano Factor

The FF is a useful count-based measure of correlation for a point process [3, 4, 7, 16]. The FF provides a direct measure of the relative clustering of a spike train over a broad range of time scales determined by the counting time. Positive correlation (relative to the benchmark Poisson point process) is dominant over those time scales where $F(T) > 1$; whereas negative correlation is dominant over time scales where $F(T) < 1$ (e.g., when refractoriness is operative). The FF is related to the autocorrelogram (coincidence rate) and to the count-based power spectral density through simple integral transforms [3, 4, 16, 30]. The Allan factor and its wavelet counterpart are closely related to the FF, and are also of use in examining long-range dependence in a point process [1, 7, 13].

Renewal Surrogate Data

Long-range correlation in a spike train can be inherent in the form of the IIH itself, or it can arise from the ordering of the sequence of intervals, or both. Randomly shuffling (reordering) the sequence of intervals of a point process provides a data set with an IIH identical to that of the original point process, but with no correlation among intervals (a renewal process). This procedure is therefore useful to determine whether the correlation that might be present in a FF arises from the form of the IIH.

This determination is made as follows:

Table 2. Characteristics of the spontaneous recordings for the four cat striate-cortex cells whose Fano factors are shown in Fig. 2. The behavior of cell 3 is examined in detail in Figs. 3 and 4.

Cell No.	Description	Duration of Recording (s)	Number of Intervals	Average Firing Rate λ (s^{-1})
4	Layer-III (complex)	6022	487	0.081
19	Layer-VI (complex)	4804	2220	0.462
7	Layer-VI (complex)	7700	13763	1.79
3	Layer-VI (complex)	1265	2300	1.82

In the limit of large counting times, a renewal process obeys:

$$F(T \to \infty) = \sigma_t^2 / \bar{t}^2 = C^2, \qquad (2)$$

where $\bar{t}$ and σ_t represent the mean and standard deviation of the IIH, respectively, and $C \equiv \sigma_t / \bar{t}$ is the coefficient of variation (CV) [33]. A shuffled data set exhibiting a FF in excess of unity for large counting times, therefore, indicates that $C > 1$. This, in turn, means that the form of the IIH for the renewal process gives rise to (at least some of) the long-duration correlation, since the zero-correlation (Poisson) renewal process has $C = 1$, which is characteristic of an exponentially distributed IIH.

Results

Using standard electrophysiological recording techniques [32, 34], nerve-spike trains were extracellularly recorded from individual cells in the striate cortex of the cat, along the medial bank of area 17. The animal was anesthetized with sodium pentothal (20 mg/kg intravenous; intraperitoneal supplementation as needed) and paralyzed with succinylcholine (10 mg/kg-h intravenous). Individual action potentials were recorded using tungsten electrodes and, after discrimination on the basis of their amplitude and time course, measured with 0.1-ms precision.

Fano Factor for Spontaneous Discharge

In Fig. 2, we display the FFs constructed from the spontaneous discharge of four different cat striate-cortex cells (solid curves). The background illumination was at a low level (about 0.25 cd/m^2) in all cases, so that the cortical firing patterns were essentially spontaneous. Cell 4 (upper-left quadrant) is a layer-III complex cell whereas cell 19 (upper-right quadrant) is a layer-VI standard complex cell [35] with a receptive field of 0.5°x2°. Cell 7 (lower-left quadrant) is a layer-VI standard complex cell with a large receptive field. Cell 3 (lower-right quadrant) is also a layer-VI standard complex cell; it is strongly contralateral monocular (left eye) and strongly directionally tuned, with a 5°x3° receptive field. The characteristics of the spontaneous recording for each cell are presented in Table 2.

The spontaneous FFs for all four cells bear a number of characteristics in common. For very short counting times ($T \lesssim 10^{-3}$ s), the FFs all assume a value close to unity. In principle, refractoriness requires that the FFs lie below unity for very short counting times; however the low spontaneous firing rates of these units renders the effects of refractoriness negligible [10, 36]. As T increases, the curves rise a bit, but they remain quite close to unity for $T \lesssim 100$ ms.

As the counting time increases further, the curves rise to values appreciably in excess of unity, but the nature of the increase differs from cell to cell. The FFs for some cells saturate at a particular counting time T that is of the order of seconds, whereas those for other cells continue to rise as the counting time becomes yet larger. As an example of the former behavior, the FF for cell 4 rises to a value of about 3 at T = 10 s and remains in that vicinity for T as large as 600 s (the FFs are only displayed to T = 40 s in Fig. 2). Of course, the longer the data set, the larger the value of T out to which the FF can be reliably determined. (As a rule of thumb, a satisfactory estimate of $F(T)$ can be ob-

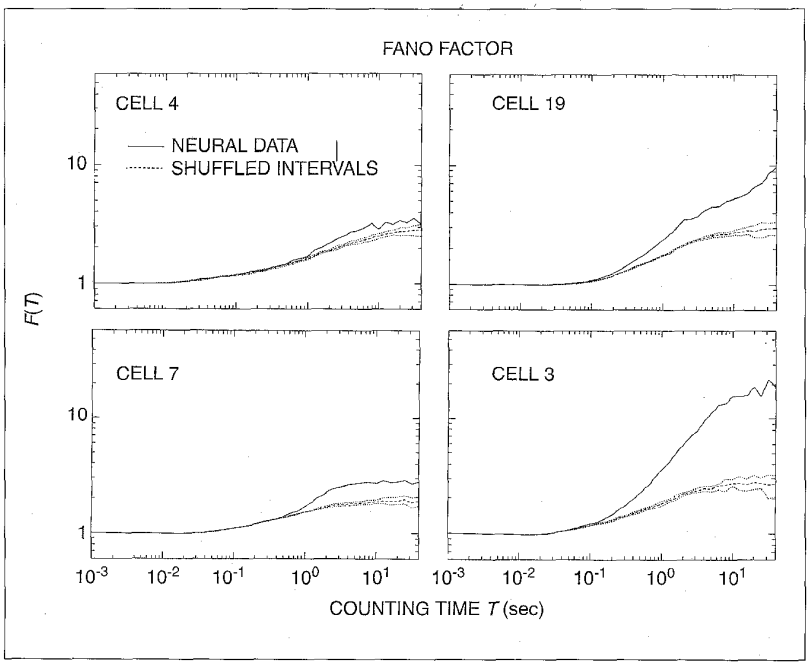

2. Fano factors (FFs) constructed from the spontaneous discharges recorded from four cat striate-cortex cells (solid curves). A description of the cell types and the characteristics of the recordings is provided in Table 2. Variance-time curves are obtained by multiplying the FFs by $\overline{N} = \lambda T$. Also shown are the mean (dashed) and the mean ± standard deviation (dotted) FFs calculated from 10 successive shufflings of the original data.

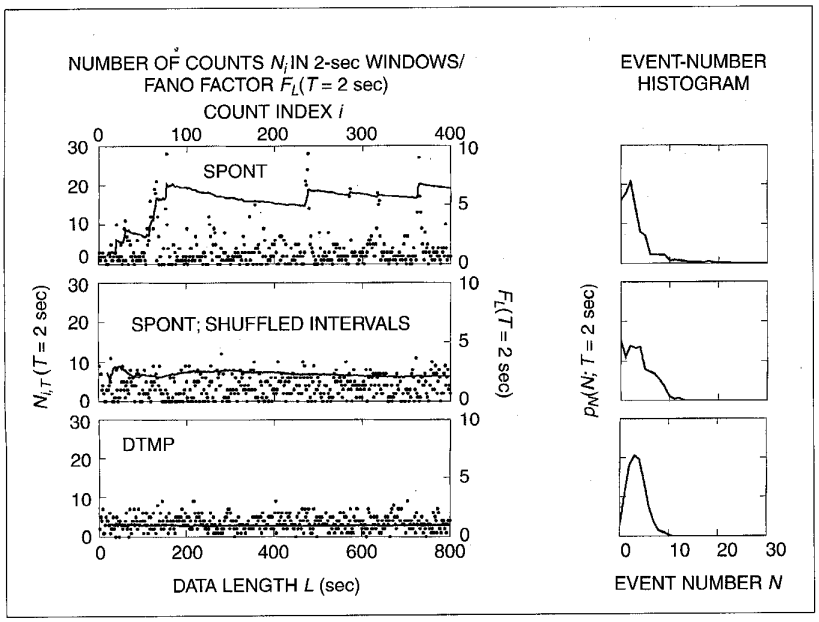

3. Sequence of counts in contiguous 2-s time windows for the spontaneous spike train from striate-cortex cell 3 (upper left panel, left ordinate, top abscissa, dots) and evolution of the Fano factor $F_L(T = 2$ s) as the length of the data set L increases (upper left panel, right ordinate, bottom abscissa, solid curve). The particular data segment illustrated extends from 400 to 1200 s after the beginning of the data set. $F_L(T = 2$ s) executes jumps when spike clusters or absences (relative to the mean) are added to the data set. The Fano factor for the entire data set is $F(T = 2$ s) ≈ 5.8. Clusters are also revealed in the large variance of the event-number histogram (ENH) associated with the entire data set (upper right panel), which has a long tail. Sequence of counts for the shuffled data (middle panel) shows the elimination of large clusters and reduction of the Fano factor. The tail in the ENH is substantially diminished. Sequence of counts for a simulated dead-time-modified Poisson point process (DTMP) of mean $\overline{N} = 3.64$ and dead time $\tau_d = 1$ msec (lower panel) shows smaller fluctuations and a FF near unity. The event-number histogram is nearly Poisson.

tained provided that $T \leq L/10$, where L is the length of the data set; $F(T)$ then comprises at least 10 samples at the largest value of T.)

The FF for cell 19, in contrast, exhibits a value of about 5 at $T = 10$ s, but continues to rise to a value in excess of 80 at $T =$ 480 s. Large FFs at large counting times are consistent with the large rate fluctuations qualitatively observed by Griffith and Horn [19] for large averaging times. They also indicate that the power-spectral density estimate of the spike train increases as frequency decreases. The FF for cell 19 resembles those observed for spontaneously firing cat RGC and LGN neurons [1, 2].

Nature of the Temporal Correlation

To ascertain whether the temporal correlation in the spike train has its origin in the form of the interevent-interval histogram or in the ordering of the sequence of intervals (or in both), we turn to the renewal surrogate data sets discussed above. The sequence of intervals of the original point process were shuffled 10 times, thereby generating an ensemble of 10 realizations of a renewal point process with an IIH identical to that of the original data. The FF was then computed for each of these surrogate data sets. The resulting mean (dashed) and mean ± standard deviation (dotted) FFs are presented in each panel of Fig. 2, along with the original unshuffled data (solid).

For all counting times greater than a few hundred ms, the original data generally lie many standard deviations above the mean FF of the renewal ensemble. This result provides a clear demonstration that the ordering of the sequence of intervals contributes to the correlation, so that the original spike train is distinctly nonrenewal in nature. Moreover, for all of the data sets that we have investigated, even the renewal (shuffled) FFs remain well above unity for large counting times. Examining the dashed curves in Fig. 2, for example, we find that $1.8 \leq F(T = 40$ sec) ≤ 3 for these four cells. Since $F(T \to \infty) = C^2$, this means that $1.3 \leq C \leq 1.7$. Because this value is greater than unity, there is positive correlation inherent in the IIH, as discussed above. Similar results have been obtained for RGC and LGN neurons at low firing rates [2].

We conclude that the correlation observed in the spontaneous striate-cortex-cell spike trains is of dual origin: the ordering of the sequence of interevent intervals and the form of the IIH itself.

Dependence of Fano-Factor Magnitude on Length of Data Set

To investigate the dependence of the FF on the length of the data set, we choose cell 3 for detailed study. The results are representative of the other striate-cortex cells we have examined and are consistent with the data collected by others.

Figure 3 illustrates the sequence of counts, N_i, for the spontaneous discharge recorded from cell 3 (upper left panel, left ordinate, top abscissa, dots) in contiguous 2-s time windows (see Fig. 1 for an explanation). The variation in the heights of the dots shows how the spike numbers in 2-s intervals wax and wane. Also plotted in the same panel is a version of the FF, $F_L(T = 2$ s), that is continuously updated as the length of the data set L increases (upper left panel, right ordinate, bottom abscissa, solid curve). Spike clustering in the data set is revealed by a sizable number of counting windows with large numbers of counts. These large-count windows often lie near each other because the counts are correlated. As expected, $F_L(T = 2$ s) executes jumps at those data lengths L when additions to the data set arise from spike clusters above the mean, or from spike absences below the mean, because such events increase variability. The FF grows in this manner until the amount of data incorporated is sufficient to insure that the large spike clusters, which occur relatively rarely, have been adequately sampled. The presence of clusters is also revealed in the event-number histogram $p_N(N; T)$ associated with the entire data set (upper right panel); the distribution has a long tail and therefore large variance.

This behavior is in general accord with the data collected by others for a fixed counting time; comparing the results in Table 1 shows that longer data sets usually

Table 3. Characteristics of four recordings from a cat striate-cortex standard-complex cell (cell 3) driven by a stimulus with different modulation periods. This particular layer-VI cell is strongly contralateral monocular (left eye), and strongly directionally tuned with a 5°x3° receptive field. The first row represents the spontaneous discharge (background level ~ 0.25 cd/m^2). The remaining three rows represent driven data; the stimulus was an illuminated light bar projected during the first half of each modulation period. The Fano-factor curves are displayed in Fig. 4.

Fig.	Modulation Period T_M (s)	Duration of Recording (s)	Number of Intervals	Average Firing Rate λ (s^{-1})
4A	spontaneous	1265	2300	1.82
4B	1.0	545	19607	36.0
4C	0.2	560	21298	38.0
4D	0.1	339	10529	31.1

have greater values of $F(T)$. It is also clear that using too few samples to compute the FF will generally result in its underestimation. This is because contiguous values of the count random variable often lie close to each other because they are correlated, as is evident in Fig. 3. Thus, the selection of specific action-potential segments for "constant firing rate," a technique used by Snowden, et al. [28], and by Softky and Koch [29], artificially reduces the variance and, therefore, the FF [11].

A similar plot for the shuffled surrogate is presented in Fig. 3 (middle panel). The large spike clusters are dissolved by the random rearrangement of the interval ordering, and the magnitude of the FF is substantially reduced. The PND loses its long tail. The residual fluctuations (above the Poisson) in this renewal process arise purely from the form of the interevent-interval histogram.

An analogous plot for a simulated dead-time-modified Poisson point process (DTMP) is presented in the lower panel of Fig. 3. In this case, the fluctuations are even smaller than those of the shuffled surrogate (the FF is very near unity) since neither correlation associated with the IIH, nor with the interval ordering, is present. The PND assumes a nearly Poisson form.

Fano Factor for Driven Discharge

We now examine the alteration in the FF for cell 3 in the presence of a stimulus. An illuminated light bar was periodically projected onto the receptive field of the cell at its optimal angle. Square-wave modulation with a 50% duty cycle was used; the stimulus was projected during the first half of the modulation period T_M while only the residual background level (~ 0.25 cd/m^2) was present during the second half. The characteristics of the recordings are summarized in Table 3. The Fano-factor curves are displayed in Fig. 4. The upper left-hand panel of Fig. 4 represents the spontaneous discharge (A), whereas the other panels represent driven data (modulation period T_M = 1.0, 0.2, and 0.1 s in B, C, and D, respectively).

The FFs for the driven and spontaneous data differ in several significant respects. The distinctions are most clearly drawn by comparing the behavior of the spontaneous curve (Fig. 4A) with the driven curve presented in Fig. 4C (T_M = 0.2 s).

The spontaneous FF in Fig. 4A remains essentially constant at unity, until it begins to slowly increase when T reaches 20 ms. The FF exceeds 2 at about T = 400 ms, indicating the onset of measurable clustering (positive temporal correlation) in the spike train. The FF continues to rise with increasing T, in this case attaining a value of 20 at a counting time of 40 s. The approximately straight-line behavior on log-log coordinates indicates power-law growth for this particular FF, mandating that the power spectral density (PSD) of the spike train exhibits 1/*f*-type behavior for frequencies below about 1/0.4 = 2.5 Hz [3, 4, 16].

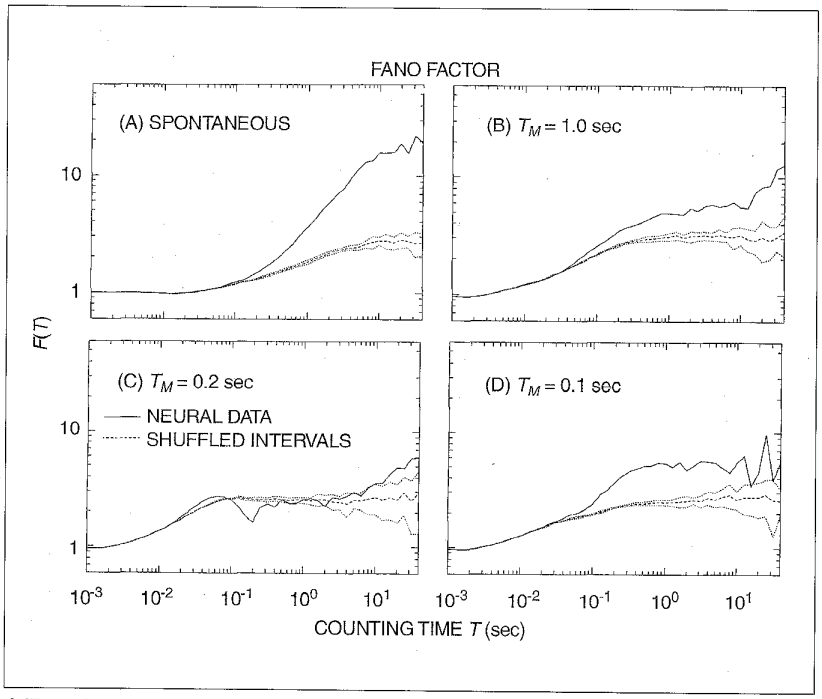

4. Fano factors (FFs) constructed from four recordings obtained from a cat striate-cortex cell (cell 3, solid curves). The characteristics of the recordings are indicated in Table 3. Also shown are the mean (dashed) and the mean ± standard deviation (dotted) FFs calculated from 10 successive shufflings of the original data. The upper left-hand panel (A) represents the spontaneous FF whereas the other panels represent driven data (modulation period T_M = 1.0, 0.2, and 0.1 s in B, C, and D, respectively). Successive-interval return maps (joint interval histograms) for these same data are presented by Siegel [32, Fig 5]. The behavior of the shuffled surrogate data sets reveals that both the ordering of the intervals, and the form of the IIH, contribute to the long-duration correlation, as with the spontaneous data.

The driven FF in Fig. 4C, on the other hand, lies just below unity for $T = 1$ ms, as a result of refractoriness. Refractoriness is not entirely negligible in the driven case because of the increased average firing rate. The driven FF rises more quickly than its spontaneous counterpart. It already exceeds 2 at $T = 20$ ms, rises to a local maximum at 70 ms, and then falls below 2 at 150 ms. It then reaches a local minimum at $T = 200$ ms, which is equal to the modulation period.

In brief, the driven FF exhibits a clear "bump" extending from about 20 to 150 ms. The linear-transform relationship between the FF and the PSD [3, 4, 16] indicates that there must, therefore, be a corresponding bump in the PSD stretching from $f = 1/0.15$ to $1/0.02$ Hz, i.e., from 6 to 50 Hz. This excess power is, no doubt, a manifestation of the quasirhythmic (so-called "40-Hz") activity that appears in striate-cortex cells when a visual stimulus is presented [37, 38].

The dip at $T \approx T_M = 0.2$ s reflects phase locking to the stimulus. Variability, and therefore the FF, is reduced when the counting time is adjusted so that it captures similar numbers of spikes on successive trials [13]. A moment's thought reveals that this happens when $T = T_M$. Although the driven FF resumes its growth for larger values of T, its value remains suppressed relative to that of the spontaneous FF, a result of the pattern imposed on the spike train by the modulated stimulus. Thus, $1/f$-type behavior of the PSD at very low-frequencies, corresponding to power-law growth of the FF at large counting times, is diminished by the presence of the stimulus.

The results presented in Fig. 4 show that the values of $F(T = \frac{1}{2}$ or 1 s) range between 2.5 and 5, which accord perfectly with the values obtained by others (see Table 1). Clearly, the form of the FF as a function of T conveys far more information than the FF value at a single counting time.

Discussion

We have quantitatively examined the spontaneous firing patterns exhibited by cat striate-cortex neurons, and the modifications of these patterns induced by the presence of a visual stimulus. We have used the FF to gain insight into the nature of the correlation present in these spike trains. Wavelet-based generalizations of the FF, and its close cousin the Allan factor [1], provide results similar to those presented here.

Cat striate-cortex FFs bear reasonable similarity to those obtained from locust DCMD interneurons.

It is of interest to compare the statistical characteristics of the striate-cortex spontaneous patterns with those of other sensory neurons for which count-based variability has been extensively studied.

Cat striate-cortex FFs bear reasonable similarity to those obtained from locust DCMD interneurons. The upper panel of Fig. 5 presents the spontaneous-discharge FFs for four cat striate-cortex cells (replotted from the solid curves in Fig. 2). The FFs for four DCMD cells are shown [10] on the same scale in the middle panel of Fig. 5. Although the two sets of FFs are rather similar, there is substantially more variability among the cortical-cell spike trains than among those from the DCMD cells. For both preparations, the growth of the FF with increasing counting time is not steady and in some cases saturates.

The lower panel of Fig. 5 displays the mean (solid) FF bracketed by one standard deviation on either side (dotted) FFs obtained from 10 simulations of a DTMP. The Poisson point process has a FF pinned at unity, whereas the DTMP remains slightly below unity as a result of the anticorrelation introduced by refractoriness [33, 36]. It is clear that both the

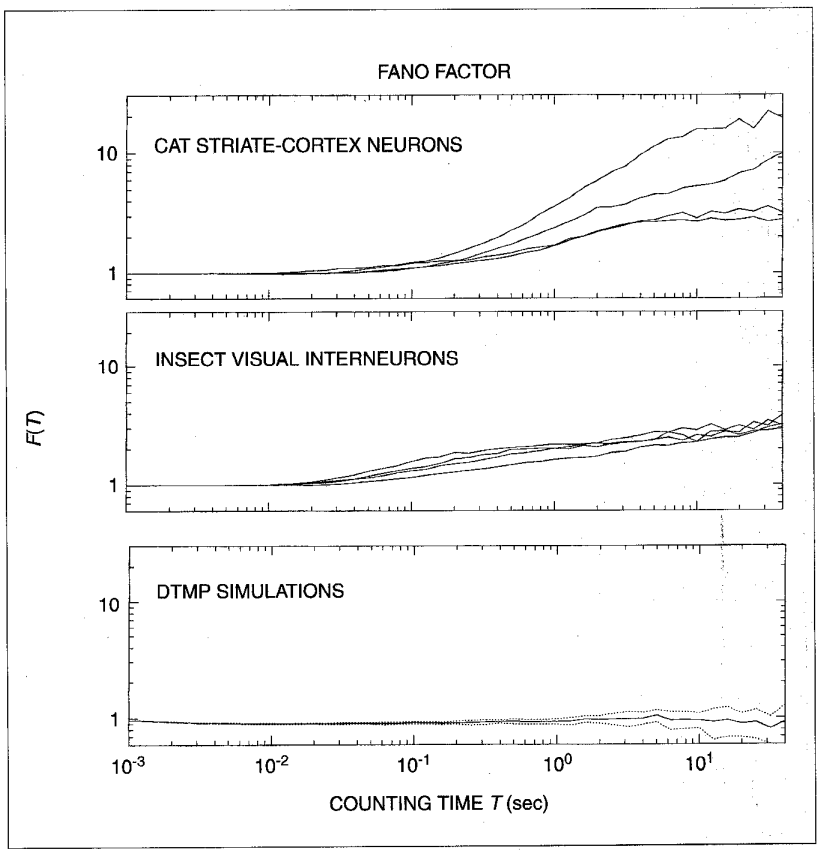

5. Comparison of FFs for the spontaneous discharge from four striate-cortex cells (upper panel, replotted from Fig. 2), and four locust DCMD visual interneurons (middle panel, after Turcott, et al. [10]). The lower panel shows the FF, along with its one-standard-deviation limits, obtained from 10 simulations of a DTMP with rate $\lambda = 36.0$ sec^{-1} and dead time $\tau_d = 1.5$ msec.

striate-cortex and the DCMD FFs reveal substantial positive correlation and are not well described by the DTMP.

Comparison of the striate-cortex FFs with those observed from primary auditory nerve fibers [4, 7] shows that although they both grow with increasing counting time, they differ in character for counting times $T > 100$ ms. The auditory FFs grow steadily, rising in fractional-power-law form out to the largest time scales permitted by the length of the data set (typically hundreds of seconds), with no hint of saturation. Another significant distinction is that the FFs for shuffled auditory neural spike trains cannot be distinguished from those arising from the DTMP, whereas the FFs for shuffled striate-cortex spike trains (see Figs. 2 and 4) retain correlations arising from the form of the IIH. The striate-cortex FFs are quite similar to those obtained from LGN cells [1, 2], in the presence of a stimulus as well as in its absence.

The sequence of action potentials at these cortical cells can likely be modeled by an integrate-and-fire construct [13] or by a doubly-stochastic point process [16] (A fractal version of such a doubly stochastic point process, the fractal binomial-noise-driven gamma-r point process (FBNDG), leads to a nonsaturating FF that grows in fractional power-law form with the counting time T, and satisfactorily describes the spontaneous neural firing patterns of cat RGC and LGN neurons [1,2]). An early suggestion along these lines was made by Smith and Smith [18]. The driving stochastic-rate process might be associated with slow cortical fluctuations [39, 40]. Indeed Hubel's [17, Figs. 3 and 4] measurements reveal that the burstiness of the cortical spike trains and the variability in the electrocorticogram increase together as the animal moves from sleep to waking and vice versa.

The biophysical locus of these fluctuations (or their transfer from one neuron to another) may reside at the synapse. Neurotransmitter packets released from the presynaptic membrane in a number of preparations form highly variable sequences that exhibit long-duration correlation [11]. A large momentary fluctuation could enhance the firing probability, thereby providing a mechanism through which the statistical (and correlation) properties of presynaptic excocytosis are transferred to a cortical-cell spike train. Mainen and Sejnowski [41] have suggested that such a transfer occurs in a neocortical neuron when it is stimulated by white Gaussian-noise current, a stimulus that is, however, devoid of correlation. How such fluctuations might relate to information transmission is a different question.

Acknowledgments

We are grateful to Dr. Torsten Wiesel for the use of his laboratory facilities in collecting the data reported here. This work was supported by the Office of Naval Research under Grant N00014-92-J-1251 to MCT and Grant N00014-93-1-0334 to RMS, and by the National Institutes of Health under grant 1R01-EY 09223 to RMS.

Malvin C. Teich (S'62-M'66-SM'72-F'89) was born in New York City. He received the S.B. degree in physics from the Massachusetts Institute of Technology, Cambridge, MA, in 1961, the M.S. degree in electrical engineering from Stanford University, Stanford, CA, in 1962, and the Ph.D. degree from Cornell University, Ithaca, NY, in 1966.

After receiving the doctorate he joined MIT Lincoln Laboratory, Lexington, MA, where he was engaged in work on coherent infrared detection. In 1967 he became a member of the faculty at Columbia University, New York. He served as a member of the Electrical Engineering Department (as Chairman from 1978 to 1980), the Applied Physics Department, and the Columbia Radiation Laboratory. He was appointed Professor Emeritus in 1996.

Dr. Teich is now teaching and pursuing his research interests at Boston University, where he is Professor in the Departments of Electrical and Computer Engineering, and Biomedical Engineering. He is working in the areas of quantum optics, photonics, fractal point processes in physical and biological systems, and information transmission in biological sensory systems. He has authored or coauthored some 200 technical publications and holds one patent. He is the coauthor of *Fundamentals of Photonics* (Wiley, 1991).

Prof. Teich was the recipient of the IEEE Browder J. Thompson Memorial Prize Award for his paper "Infrared Heterodyne Detection" in 1969, and in 1981 he received the Citation Classic Award of the Institute for Scientific Information for this work. He was awarded a Guggenheim Fellowship in 1973. In 1992 he was honored with the Memorial Gold Medal of Palacký University in the Czech Republic. He is a Fellow of the American Physical Society, the Optical Society of America, the Institute of Electrical and Electronics Engineers, the American Association for the Advancement of Science, and the Acoustical Society of America. He is a member of Sigma Xi, Tau Beta Pi, the Association for Research in Otolaryngology, and the Biomedical Engineering Society.

Prof. Teich served as a member of the Editorial Advisory Panel for the journal *Optics Letters* from 1977 to 1979, as a Member of the Editorial Board of the *Journal of Visual Communication and Image Representation* from 1989 to 1992, and as Deputy Editor of *Quantum Optics* from 1988 to 1994. He is currently a Member of the Editorial Board of the journal *Jemná Mechanika a Optika* and a Member of the Advisory Board of the IEEE Press Series *Emerging Technologies in Biomedical Engineering*. He is a Member of the Scientific Board of the Czech Academy of Sciences' Institute of Physics.

Robert G. Turcott (S'88) was born in Seattle, WA. He received the B.S. degree in electrical engineering from Columbia University in 1985. He then moved to Kyoto, Japan for two years, where he studied language and culture. After returning to Columbia, he received the M.S. and Ph.D. degrees in electrical engineering in 1990 and 1994, respectively. His research interests include information representation and processing by neural systems, signal-based diagnostic algorithms, and mechanisms of cardiac arrhythmias. He is currently a research consultant in the biomedical industry, and a medical student at Stanford University.

Ralph M. Siegel was born in New York City. He received the B.Sc. degree in physics in 1979 and the Ph.D. degree in physiology in 1984, both from McGill University, Montreal, Quebec. His doctoral work involved the characterization of

electrogenic sodium-potassium exchange in unmyelinated nerve fibers.

After receiving the doctorate, he joined the Developmental Neurobiology Laboratory at the Salk Institute for Biological Studies, La Jolla, CA, where he worked as a post-doctoral fellow with Richard Andersen, using single-unit recording techniques to study the representation of extra-personal visual space in the behaving monkey. He also conducted psychophysical studies of motion perception on human and nonhuman primates. In 1988, he joined Torsten Wiesel's Laboratory of Neurobiology at Rockefeller University in New York City, where he continued his studies of motion perception and began investigating the dynamical properties of neurons in the primary visual cortex.

In 1989, he became a member of the graduate faculty at the interdisciplinary Center for Molecular and Behavioral Neuroscience, Rutgers University, Newark, NJ, where he is now teaching and pursuing his research interests in the perception of space and form from motion by behaving monkeys, as well as neural models of perception and chaos theory.

Address for Correspondence: *Dr. Teich*: Department of Electrical and Computer Engineering, Boston University, 44 Cummington Street, Boston, MA 02215-2407. E-mail: teich@bu.edu; *Dr. Turcott*: 3131 Goodwin Avenue, Redwood City, CA 94061. E-mail: turcott@leland.stanford.edu; *Dr. Siegel*: Center for Molecular and Behavioral Neuroscience, Rutgers University, 197 University Avenue, Newark, NJ 07102. E-mail: axon@cortex.rutgers.edu

References

1. **Teich MC, Heneghan C, Lowen SB, Turcott RG:** Estimating the fractal exponent of point processes in biological systems using wavelet- and Fourier-transform methods. In: Aldroubi A and Unser M (eds) *Wavelets in medicine and biology*. CRC Press, Boca Raton, FL, 1996, pp. 383-412.

2. **Teich MC, Heneghan C, Lowen SB, Ozaki T, Kaplan E:** Fractal character of the neural spike train in the visual system of the cat. *J Opt Soc Am*, in press, 1996.

3. **Teich MC:** Fractal character of the auditory neural spike train. *IEEE Trans Biomed Eng* 36:150-160, 1989.

4. **Teich MC:** Fractal neuronal firing patterns. In: McKenna T, Davis J, and Zornetzer S (eds) *Single neuron computation*. Academic, Boston, pp 589-625, 1992.

5. **Kumar AR, Johnson DH:** Analyzing and modeling fractal intensity point processes. *J Acoust Soc Am* 93:3365-3373, 1993.

6. **Kelly OE, Johnson DH, Delgutte B, Cariani P:** Fractal noise strength in auditory-nerve fiber recordings. *J Acoust Soc Am* 99:2210-2220, 1996.

7. **Lowen SB, Teich MC:** The periodogram and Allan variance reveal fractal exponents greater than unity in auditory-nerve spike trains. *J Acoust Soc Am* 99:3585-3591, 1996.

8. **Powers NL, Salvi RJ, Saunders SS:** Discharge rate fluctuations in the auditory nerve of the chinchilla, *Abstracts of the XIV Midwinter Research Meeting, Assoc for Res in Otolaryngology*, Des Moines, IA, Abstract No. 411, p. 129, 1991.

9. **Powers NL, Salvi RJ:** Comparison of discharge rate fluctuations in the auditory nerve of chickens and chinchillas, *Abstracts of the XV Midwinter Research Meeting, Assoc for Res in Otolaryngology*, Des Moines, IA, Abstract No. 292, p. 101, 1992.

10. **Turcott RG, Barker PDR, Teich MC:** Long-duration correlation in the sequence of action potentials in an insect visual interneuron. *J Statist Comput Simul* 52:253-271, 1995.

11. **Lowen SB, Cash SS, Poo M-m, Teich MC:** Quantal neurotransmitter secretion exhibits fractal behavior. *J Neurosci*, submitted, 1996.

12. **Turcott RG, Teich MC:** Long-duration correlation and attractor topology of the heartbeat rate differ for normal patients and those with heart failure. *Proc SPIE* 2036:22-39, 1993.

13. **Turcott RG, Teich MC:** Fractal character of the electrocardiogram: distinguishing heart-failure and normal patients. *Ann Biomed Eng* 24:269-293, 1996.

14. **Teich MC, Khanna SM:** Pulse-number distribution for the neural spike train in the cat's auditory nerve. *J Acoust Soc Am* 77:1110-1128, 1985.

15. **Fano U:** Ionization yield of radiations. II. The fluctuations of the number of ions. *Phys Rev* 72:26-29, 1947.

16. **Lowen SB, Teich MC:** Estimation and simulation of fractal stochastic point processes. *Fractals* 3:183-210, 1995.

17. **Hubel DH:** Single unit activity in striate cortex of unrestrained cats. *J Physiol (London)* 147:226-238, 1959.

18. **Smith DR, Smith GK:** A statistical analysis of the continual activity of single cortical neurones in the cat unanesthetized isolated forebrain. *Biophys J* 5:47-74, 1965.

19. **Griffith JS, Horn G:** An analysis of spontaneous impulse activity of units in the striate cortex of unrestrained cats. *J Physiol (London)* 186:516-534, 1966.

20. **Sanseverino ER, Agnati LF, Maioli MG, Galletti C:** Maintained activity of single neurons in striate and non-striate areas of the cat visual cortex. *Brain Res* 54:225-242, 1973.

21. **Schiller PH, Finlay BL, Volman SF:** Short-term response variability of monkey striate neurons. *Brain Res* 105:347-349, 1976.

22. **Tolhurst DJ, Movshon JA, Thompson ID:** The dependence of response amplitude and variance of cat visual cortical neurones on stimulus contrast. *Exp Brain Res* 41:414-419, 1981.

23. **Dean AF:** The variability of discharge of simple cells in the cat striate cortex. *Exp Brain Res* 44:437-440, 1981.

24. **Tolhurst DJ, Movshon JA, Dean AF:** The statistical reliability of signals in single neurons in cat and monkey visual cortex. *Vision Res* 23:775-785, 1983.

25. **Legéndy CR, Salcman M:** Bursts and recurrences of bursts in the spike trains of spontaneously active striate cortex neurons. *J Neurophysiol* 53:926-939, 1985.

26. **Bradley A, Skottun BC, Ohzawa I, Sclar G, Freeman RD:** Visual orientation and spatial frequency discrimination: a comparison of single neurons and behavior. *J Neurophysiol* 57:755-772, 1987.

27. **Vogels R, Spileers W, Orban GA:** The response variability of striate cortical neurons in the behaving monkey. *Exp Brain Res* 77:432-436, 1989.

28. **Snowden RJ, Treue S, Andersen RA:** The response of neurons in areas V1 and MT of the alert rhesus monkey to moving random dot patterns. *Exp Brain Res* 88:389-400, 1992.

29. **Softky WR, Koch C:** The highly irregular firing of cortical cells is inconsistent with temporal integration of random EPSPs. *J Neurosci* 13:334-350, 1993.

30. **Cox DR, Lewis PAW:** *The statistical analysis of series of events*. Chapman and Hall, London, 1966.

31. **Rodieck RW, Kiang NY-S, Gerstein GL:** Some quantitative methods for the study of spontaneous activity of single neurons. *Biophys J* 2:351-368, 1962.

32. **Siegel RM:** Non-linear dynamical system theory and primary visual cortical processing. *Physica D* 42:385-395, 1990.

33. **Parzen E:** *Stochastic processes*. Holden-Day, San Francisco, 1962, p. 180.

34. **Hubel DH, Wiesel TN:** Functional architecture of Macaque monkey visual-cortex. *Proc R Soc London Ser B* 198:1-59, 1977.

35. **Gilbert CD:** Laminar differences in receptive field properties of cells in cat primary visual cortex. *J Physiol (London)* 268: 391-421, 1977.

36. **Teich MC, Matin L, Cantor BI:** Refractoriness in the maintained discharge of the cat's retinal ganglion cell. *J Opt Soc Am* 68:386-402, 1978.

37. **Gray CM, Singer W:** Stimulus-specific neuronal oscillations in orientation columns of cat visual cortex. *Proc Nat Acad Sci* 86:1698-1702, 1989.

38. **Gray CM:** Synchronous oscillations in neuronal systems: mechanisms and functions. *J Comp Neurosci* 1:11-38, 1994.

39. **Robertson ADJ:** Correlation between unit activity and slow potential changes in the unanaesthetised cerebral cortex of the cat. *Nature* 208:757-758, 1965.

40. **Tomko GJ, Crapper DR:** Neuronal variability: non-stationary responses to identical visual stimuli. *Brain Res* 79:405-418, 1974.

41. **Mainen ZF, Sejnowski TJ:** Reliability of spike timing in neocortical neurons. *Science* 268:1503-1506, 1995.